Manganese Citrate Chemistry: Syntheses, Spectroscopic Studies, and Structural Characterizations of Novel Mononuclear, Water-Soluble Manganese Citrate Complexes

M. Matzapetakis,[†] N. Karligiano,[‡] A. Bino,[‡] M. Dakanali,[†] C. P. Raptopoulou,[§] V. Tangoulis,[§] A. Terzis,[§] J. Giapintzakis,[||] and A. Salifoglou*[,†]

Department of Chemistry, University of Crete, Heraklion 71409, Greece, Department of Inorganic and Analytical Chemistry, The Hebrew University of Jerusalem, 91904 Jerusalem, Israel, Institute of Materials Science, NCSR "Demokritos", 15310 Aghia Paraskevi, Attiki, Greece, and Institute of Electronic Structure and Laser, Foundation for Research and Technology−Hellas, 71110 Heraklion, Greece

Received October 26, 1999

The first two mononuclear manganese citrate complexes, $(NH_4)_4[Mn^{II}(C_6H_5O_7)_2]$ (**1**) and $(NH_4)_5[Mn^{III}(C_6H_4O_7)_2]\cdot 2H_2O$ (**2**) were synthesized in aqueous solutions near physiological pH values. They were isolated in their pure crystalline forms and characterized by elemental analyses and spectroscopic techniques, including UV/visible, electron paramagnetic resonance, Fourier transformed infrared, and magnetic susceptibility measurements. Compound **1** crystallizes in the monoclinic space group $P2_1/c$, with $a = 8.777(1)$ Å, $b = 13.656(3)$ Å, $c = 9.162(2)$ Å, $\beta = 113.62(2)°$, $V = 1006.2(6)$ Å^3, and $Z = 2$. Compound **2** crystallizes in the triclinic space group $P\bar{1}$, with $a = 9.606(3)$ Å, $b = 9.914(3)$ Å, $c = 7.247(3)$ Å, $\alpha = 91.05(1)°$, $\beta = 105.60(1)°$, $\gamma = 119.16(1)°$, $V = 571.3(3)$ Å^3, and $Z = 1$. The X-ray crystal structures of **1** and **2** revealed that, in both cases, the manganese ion is six-coordinate and is bound by two citrate ligands in a distorted octahedral fashion. In the case of complex **1**, the citrate ion binds to Mn^{2+} as a triply deprotonated ligand, retaining the central carbon hydroxyl hydrogen, whereas, in the case of compound **2**, the citrate ligand coordinates to Mn^{3+} as a fully deprotonated entity. Compound **2** contains water molecules of crystallization in the unit cell which, through extensive hydrogen-bonding interactions, bestow considerable stability upon the Mn^{3+}−citrate assembly. There are significant contributions to the stabilities of the assembled lattices in **1** and **2** arising from the ammonium counterions neutralizing the high anionic charges of the complexes. The EPR spectra attest to the presence of paramagnetic Mn^{2+} and Mn^{3+} species in the solid state. Corroborative evidence is obtained from the magnetic susceptibility measurements in the range 5−300 K. Complexes **1** and **2** present clear cases of mononuclear manganese citrate species relevant to manganese speciation in biological media and potentially related to the beneficial as well as toxic effects of manganese on humans.

Introduction

Citric acid and its numerous physiological roles[1] dominate the biochemical loci in bacteria as well as higher organisms. The ubiquity of citric acid in the carbohydrate metabolism,[2] in the citric acid cycle as a substrate,[3] in mutant forms of the nitrogenase enzyme as an organic ligand,[4] in aconitase enzymes,[5] and in other biological systems earmarks its significance as an organic cofactor. Outstanding among the roles of the citrate ion is its solubilization of metal ions, which enhances their bioavailability and subsequent absorption by biological tissues.[6] This prominent function of the citrate ion is directly related to its metal-chelating capacity, which is manifested in its multimodal coordination to various metal ions of biological significance. Such ions include iron, calcium, magnesium, zinc, nickel, and manganese. Of these, manganese has been identified as a key metal ion involved in the active sites of essential metalloenzymes related to physiological protective metabolic functions.[7] Thus, its biological role has been greatly enhanced by its direct involvement as an essential trace element[8] in functionally critical enzymes such as catalases[9] and the mitochondrial enzymes superoxide dismutase and pyruvate carboxylase as well

* To whom correspondence should be addressed. Tel: +30-81-393-652. Fax: +30-81-392-601. E-mail: salif@chemistry.uch.gr.
[†] University of Crete.
[‡] The Hebrew University of Jerusalem.
[§] NCSR "Demokritos".
[||] Foundation for Research and Technology−Hellas.

(1) (a) Glusker, J. P. *Acc. Chem. Res.* **1980**, *13*, 345−352. (b) Etcheverry, S. B.; Apella, M. C.; Baran, E. J. *J. Inorg. Biochem.* **1984**, *20*, 269−274. (c) Martin, R. B. *J. Inorg. Biochem.* **1986**, *28*, 181−187.
(2) Hamilton, E. M. N.; Gropper, S. A. S. *The Biochemistry of Human Nutrition*; West Publishing Co.: St. Paul, MN, 1987; p 117.
(3) Lippard, S. J.; Berg, J. M. *Principles of Bioinorganic Chemistry*; University Science Books: Mill Valley, CA, 1994; pp 349−378.
(4) Liang, J.; Madden, M.; Shah, V. K.; Burris, R. H. *Biochemistry* **1990**, *29*, 8577−8581.
(5) (a) Beinert, H. *FASEB J.* **1990**, *4*, 2483−2491. (b) Beinert, H.; Kennedy, M. C. *Eur. J. Biochem.* **1989**, *186*, 5−15.
(6) (a) Baker, E. N.; Baker, H. M.; Anderson, B. F.; Reeves, R. D. *Inorg. Chim. Acta* **1983**, *78*, 282−285 and references therein. (b) Lönnerdal, B.; Stanislowski, A. G.; Hurley, L. S. *J. Inorg. Biochem.* **1980**, *12*, 71−78.
(7) (a) Davis, C. D.; Greger, J. L. *Am. J. Clin. Nutr.* **1992**, *55*, 747−752. (b) Ji, L. L.; Stratman, F. W.; Lardy, H. A. *J. Am. Coll. Nutr.* **1992**, *11*, 79−86.
(8) Chappuis, P.; Poupon, J.; Arnaud, J. In *Trace Elements and Free Radicals in Oxidative Diseases*; Favier, A. E., Neve, J., Faure, P., Eds.; AOCS Press: Champaign, IL, 1994; p 46.
(9) (a) Penner-Hahn, J. E. In *Manganese Redox Enzymes*; Pecoraro, V. L., Ed.; Verlag Chemie: New York, 1992; p 29. (b) Kono, Y.; Fridovich, I. *J. Biol. Chem.* **1983**, *258*, 13646−13648. (c) Kono, Y.; Fridovich, I. *J. Biol. Chem.* **1983**, *258*, 6015−6019. (d) Allgood, G. S.; Perry, J. J. *J. Bacteriol.* **1986**, *168*, 563−567. (e) Barynin, V. V.; Grebenko, A. *Dokl. Akad. Nauk. SSSR* **1986**, *286*, 461.

10.1021/ic9912631 CCC: $19.00
Published on Web 08/11/2000

as the glial-specific enzyme glutamine synthetase.[10] Moreover, the participation of manganese in the oxygen-evolving complex of photosystem II (PSII) has been proven to be unequivocal and quintessential.[10,11] In an as yet debatable and often unclear manner, manganese has also been associated with metabolic pathways exemplifying its ability to cross the blood−brain barrier and enter the central nervous system (CNS).[10a] It has been argued that, as such, it can emerge as a neurotoxicant related to a number of physiological impairments, including neurodegenerative diseases. In this context, manganism and Parkinson's disease are among the pathological aberrations reported to have links with manganese's neurotoxic effects.[12]

Even though a plethora of studies have so far focused on various manganese−carboxylate complexes[11,13] relating to metalloclusters in proteins and enzymes, the number of reported low molecular weight manganese species bearing the physiologically prominent tricarboxylic citric acid has been meager. Research efforts targeting manganese−citrate species have resulted in the isolation and structural characterization of a polymeric manganese complex having the formula $[Mn^{II}(H_2O)_6][Mn^{II}(C_6H_5O_7)(H_2O)]_2 \cdot 2H_2O$.[14] Until our work reported here, no low molecular weight, water-soluble manganese−citrate complexes had been synthesized, isolated, or characterized.

The need to understand (a) the speciation and interaction of the manganese ion with the biologically relevant citrate ligand in aqueous media and (b) the ability of the citrate ion as an organic cofactor to efficiently mobilize this essential trace element and enhance its availability to biological sites prompted us to pursue the underlying synthetic chemistry between the two reactants in aqueous solutions. We report herein the syntheses, isolations, and spectroscopic and structural characterizations of the first mononuclear manganese citrate complexes in aqueous solutions. In view of the aforementioned advantageous as well as deleterious aspects of manganese biochemical involvement in physiological processes and impairments, such species might be relevant to that metal ion's speciation and role(s) in human metabolism and general pathophysiology.

Experimental Section

Materials and Methods. All manipulations were carried out in the open air. $MnCO_3$, $Mn(NO_3)_2 \cdot 4H_2O$, and NH_4OH were purchased from Fluka, and nanopure water was used for all reactions.

Table 1. Summary of Crystal, Intensity Collection, and Refinement Data for **1** and **2**

	1	**2**
formula	$C_{12}H_{26}MnN_4O_{14}$	$C_{12}H_{32}MnN_5O_{16}$
fw	505.31	557.37
T, K	295	298
λ(Mo Kα), Å	0.710 73	0.710 73
a, Å	8.777(1)	9.606(3)
b, Å	13.656(3)	9.914(3)
c, Å	9.162(2)	7.247(3)
α, deg		91.05(1)
β, deg	113.6(2)	105.60(1)
γ, deg		119.16(1)
V, Å^3	1006.2(6)	571.3(3)
Z	2	1
space group	$P2_1/c$	$P\bar{1}$
D_{calcd}, Mg m^{-3}	1.668	1.620
μ, mm^{-1}	0.737	0.664
octants collected	$\pm h,+k,+l$	$-h,\pm k,\pm l$
GOF	1.039	1.059
R1/wR2[a]	0.0356/0.0903[b]	0.0311/0.0829[c]

[a] $R1 = \sum||F_o| - |F_c||/\sum|F_o|$; $wR2 = [\sum w(F_o^2 - F_c^2)^2/\sum w(F_o^2)^2]^{1/2}$. [b] For 1999 reflections with $I > 2\sigma(I)$. [c] For 2048 reflections with $I > 2\sigma(I)$.

Physical Measurements. Electronic spectra were recorded on a Perkin-Elmer Lambda 6 UV/vis spectrophotometer in the range 200−900 nm, and FT-infrared measurements were obtained on a Perkin-Elmer 1760X FT-infrared spectrometer. Elemental analyses were performed by Quantitative Technologies, Inc. Magnetic susceptibility measurements were performed with a SQUID susceptometer, and EPR measurements were recorded on a Bruker ER 200D-SRC X-band spectrometer equipped with an Oxford ESR 9 cryostat at 9.174 GHz and 10 dB.

Syntheses. (a) $(NH_4)_4[Mn(C_6H_5O_7)_2]$ (1). $MnCO_3$ (0.50 g, 4.35 mmol) and citric acid monohydrate (1.80 g, 8.57 mmol) were added to 5 mL of H_2O, and the reaction mixture was refluxed overnight. On the following day, the pH of the reaction slurry was carefully adjusted to ∼7.0 by adding aqueous NH_4OH (1:1). When the mixture was allowed to stand at 4 °C, colorless crystals of $(NH_4)_4[Mn(C_6H_5O_7)_2]$ precipitated. These were collected by filtration and dried in vacuo. Yield: 1.53 g (70%). Anal. Calcd for **1**, $(NH_4)_4[Mn(C_6H_5O_7)_2]$ ($C_{12}H_{26}N_4O_{14}Mn$, MW = 505.29): C, 28.52; H, 5.19; N, 11.09. Found: C, 28.24; H, 5.33; N, 11.09.

(b) $(NH_4)_5[Mn(C_6H_4O_7)_2] \cdot 2H_2O$ (2). $Mn(NO_3)_2 \cdot 4H_2O$ (0.20 g, 0.8 mmol) was dissolved in 10 mL of nanopure water, and citric acid monohydrate (0.25 g, 1.2 mmol) was added. The resulting reaction mixture was heated to 50 °C overnight under continuous stirring. On the following day, the reaction mixture was taken to dryness. Upon dissolution of the residue in water, the pH was adjusted to ∼8 with aqueous NH_4OH (1:1), yielding a brown solution, which was subsequently allowed to stand at 4 °C. Addition of ethanol resulted in the formation of a brown crystalline material in ∼1 week. The product was isolated by filtration and dried in vacuo. Yield: 0.25 g (56%). Anal. Calcd for **2**, $(NH_4)_5[Mn(C_6H_4O_7)_2] \cdot 2H_2O$ ($C_{12}H_{32}N_5O_{16}Mn$, MW = 557.37): C, 25.85; H, 5.75; N, 12.57. Found: C, 25.73; H, 5.69; N, 12.25.

X-ray Crystallography. A colorless crystal of **1** (0.10 × 0.15 × 0.30 mm) was mounted on a glass fiber, and a brown crystal of **2** (0.20 × 0.30 × 0.50 mm) was mounted in a capillary. Intensity data for **1** and **2** were collected at room temperature on a Philips PW 1100 and a Crystal Logic dual-goniometer diffractometer, respectively, using graphite-monochromated Mo Kα radiation (λ = 0.710 73 Å). The unit cell dimensions of **1** were obtained by a least-squares fit of 24 reflections in the range $12° < \theta < 16°$, while for **2** the angular settings of 25 automatically centered reflections in the range $11° < 2\theta < 23°$ were used. The results are given in Table 1, along with other crystallographic details. Intensity data were recorded using $\theta-2\theta$ scans, to $2\theta_{max} = 55°$ for **1** and to $2\theta_{max} = 56°$ for **2**. Data for **1** were corrected for Lorentz and polarization effects, and absorption corrections were applied by using the empirical absorption program DIFABS, incorporated into

(10) (a) Aschner, M In *Metals and Oxidative Damage in Neurological Disorders*; Connor, J. R., Ed.; Plenum Press: New York, 1997; Chapter 5, pp 77−130. (b) Prohaska, J. R. *Physiol. Rev.* **1987**, *67*, 858−901. (c) Wedler, F. C. In *Progress in Medicinal Chemistry*; Ellis, G. P., Luskombe, D. K., Ed.; Elsevier Science: Amsterdam, 1993; Vol. 30, pp 89−133.

(11) (a) Pecoraro, V. L. In *Manganese Redox Enzymes*; Pecoraro, V. L., Ed.; Verlag Chemie: New York, 1992. (b) Pecoraro, V. L.; Baldwin, M. J.; Gelasco, A. *Chem. Rev.* **1994**, *94*, 807. (c) Dismukes, G. C. *Chem. Rev.* **1996**, *96*, 2909. (d) Yachandra, V. K.; Sauer, K.; Klein, M. P. *Chem. Rev.* **1996**, *96*, 7.

(12) (a) Calne, D. B.; Chu, N. S.; Huang, C. C.; Lu, C. S.; Olanow, W. *Neurology* **1994**, *44*, 1583−1586. (b) Chia, S. E.; Foo, S. C.; Gan, S. L.; Jeratnam, J.; Tian, C. S. *Scand. J. Work, Environ. Health* **1993**, *19*, 264−270. (c) Florence M. In *Proceedings of the Workshop on Bioavailability and Oral Toxicity of Manganese*; Velasquez, S., Ed.; U.S. EPA: Washington, DC, 1995; pp 83−94.

(13) (a) Wieghardt, K. *Angew. Chem., Int. Ed. Engl.* **1994**, *33*, 725−728. (b) Proserpio, D. M.; Rappe, K. A.; Gorun, S. M. *Inorg. Chim. Acta* **1993**, *213*, 319−324 and references therein. (c) Christou, G. *Acc. Chem. Res.* **1989**, *22*, 328−335. (d) Webber, A. N.; Spencer, L.; Sawyer, D. T.; Heath, R. L. *FEBS Lett.* **1985**, *189*, 258−262. (e) Yamaguchi, K.; Sawyer, D. T. *Inorg. Chem.* **1985**, *24*, 971−976. (f) Sawyer, D. T.; Bodini, M. E. *J. Am. Chem. Soc.* **1975**, *97*, 6588−6590.

(14) Carrell, H. L.; Glusker, H. P. *Acta Crystallogr., Sect. B* **1973**, *29*, 638−640.

TEXSAN.[15] For **2**, Lorentz, polarization, and ψ-scan absorption corrections were applied by using Crystal Logic software. The heavy-atom position in **1** was obtained from a three-dimensional Patterson function, while the structure of **2** was solved by direct methods using SHELXS-86.[16] Both structures were refined by full-matrix least-squares techniques on F^2 with SHELXL-93.[16] All hydrogen atoms were located by difference maps and refined isotropically; all non-H atoms were refined anisotropically. In **1**, both ammonium counterions in the unit cell are sitting on general positions. One of the ammonium counterions in **2** is sitting disordered on a center of symmetry, and only two of its hydrogens were included in the refinement. The other two ammonium counterions in the unit cell are sitting on general positions. Experimental crystallographic details for **1**: data collected/unique/used, 2419/2290 (R_{int} = 0.0200)/2290; parameters refined, 194; $(\Delta\rho)_{max}/(\Delta\rho)_{min}$ = 0.327/−0.337 e/Å^3; $(\Delta/\sigma)_{max}$ = 0.001; R1/wR2 (for all data) = 0.0422/0.0933. Experimental crystallographic details for **2**: data collected/unique/used, 2304/2140 (R_{int} = 0.0056)/2140; parameters refined, 222; $(\Delta\rho)_{max}/(\Delta\rho)_{min}$ = 0.603/−0.375 e/Å^3; $(\Delta/\sigma)_{max}$ = 0.007; R1/wR2 (for all data) = 0.0325/0.0844.

Results

Syntheses. Simple procedures (reactions 1 and 2) were employed to synthesize the desired complexes **1** and **2**. In both cases, Mn^{2+} and citric acid in a 1:2 molar ratio were used to initiate the reactions in aqueous solutions. Subsequent manipulations of the reaction mixtures proved to be pivotal in forming the Mn^{2+} bis(citrate) complex and its oxidized analogue. Adjustment of the pH values of both reaction mixtures was accomplished with NH_4OH. Use of this reagent as a base—under the different synthetic conditions—not only provided the basic environment for the generation of the anionic forms of citrate but also supplied the necessary counterions to balance the negative charges of the title complexes: 4− for the Mn^{2+} and 5− for the Mn^{3+} bis(citrate) complex anion. In the case of **2**, following treatment of the reaction mixture as described above, the use of NH_4OH to raise the pH to ∼8 resulted in a color change of the solution to an oily brown, signifying oxidation of Mn^{2+} to Mn^{3+}. Therefore, it appears that the pH is a very critical factor in determining the oxidation state of manganese in the citrate complex synthesis reactions (eqs 1 and 2) carried

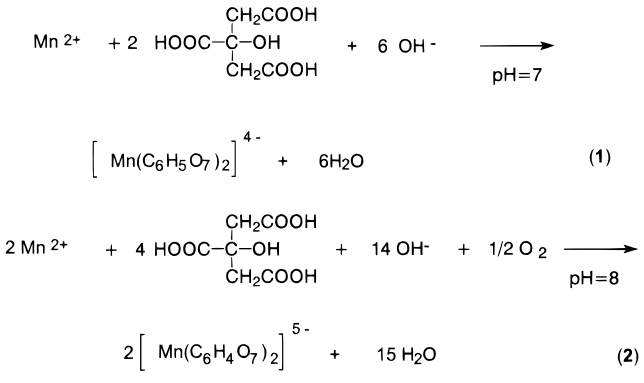

out under the aforementioned conditions. Crystalline products in fairly high yields were obtained in both cases at 4 °C. Elemental analyses of **1** and **2** led to their formulations as $(NH_4)_4[Mn(C_6H_5O_7)_2]$ (**1**) and $(NH_4)_5[Mn(C_6H_4O_7)_2]\cdot 2H_2O$ (**2**). Both **1** and **2** crystalline solids have proven to be stable in the air for long periods of time (months) without any visible signs of decomposition, and both materials are soluble in aqueous solutions at pH ∼7.

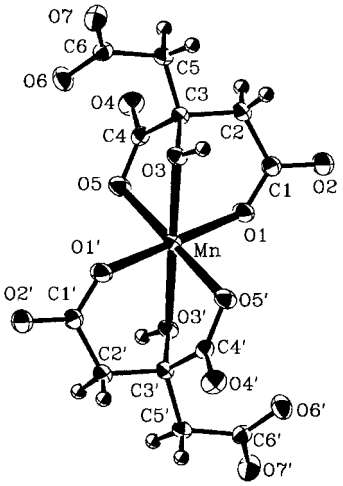

Figure 1. Structure of the $[Mn(C_6H_5O_7)_2]^{4-}$ anion in **1**, along with the atom-labeling scheme. Thermal ellipsoids were drawn by ORTEP and represent 50% probability surfaces.

Table 2. Bond Lengths (Å) and Angles (deg) for **1** and **2**

	1	**2**
Mn−O(1)	2.117(2)	2.2244(14)
Mn−O(3)	2.225(2)	1.8850(13)
Mn−O(5)	2.162(2)	1.9452(14)
O(1)−C(1)	1.265(3)	1.269(2)
O(3)−C(3)	1.444(2)	1.427(2)
O(5)−C(4)	1.281(2)	1.292(2)
C(1)−O(2)	1.245(3)	1.246(2)
C(1)−C(2)	1.513(3)	1.520(3)
C(2)−C(3)	1.543(3)	1.538(2)
C(3)−C(5)	1.537(3)	1.529(2)
C(3)−C(4)	1.544(3)	1.544(2)
C(4)−O(4)	1.231(2)	1.231(2)
C(5)−C(6)	1.520(3)	1.520(3)
C(6)−O(6)	1.246(3)	1.258(3)
C(6)−O(7)	1.262(2)	1.240(3)
O(1)−Mn−O(3)	83.04(5)	86.70(5)
O(5)−Mn−O(3)	72.47(5)	83.98(6)
O(1)−Mn−O(5)	87.01(6)	86.86(6)
C(1)−O(1)−Mn	133.41(14)	127.29(12)
C(3)−O(3)−Mn	107.57(10)	109.04(10)
C(4)−O(5)−Mn	113.16(12)	110.84(11)
O(2)−C(1)−O(1)	122.1(2)	123.4(2)
O(2)−C(1)−C(2)	118.1(2)	117.1(2)
O(1)−C(1)−C(2)	119.9(2)	119.5(2)
C(1)−C(2)−C(3)	117.9(2)	116.24(14)
O(3)−C(3)−C(5)	109.9(2)	109.81(14)
O(3)−C(3)−C(2)	110.5(2)	110.06(14)
C(5)−C(3)−C(2)	107.9(2)	108.37(14)
O(3)−C(3)−C(4)	107.7(2)	108.34(13)
C(5)−C(3)−C(4)	111.9(2)	112.6(2)
C(2)−C(3)−C(4)	109.0(2)	107.62(14)
O(4)−C(4)−O(5)	124.3(2)	122.6(2)
O(4)−C(4)−C(3)	118.2(2)	121.8(2)
O(5)−C(4)−C(3)	117.4(2)	115.3(2)
C(6)−C(5)−C(3)	115.9(2)	115.6(2)
O(6)−C(6)−O(7)	123.1(2)	124.6(2)
O(6)−C(6)−C(5)	118.7(2)	115.9(2)
O(7)−C(6)−C(5)	118.1(2)	119.3(2)

X-ray Crystallographic Structures. (a) $[Mn(C_6H_5O_7)_2]^{4-}$ (1). Single-crystal X-ray crystallographic analysis revealed that complex **1** crystallizes in the monoclinic space group $P2_1/c$ with 2 molecules in the unit cell. The structure consists of discrete $[Mn(C_6H_5O_7)_2]^{4-}$ anions with the ORTEP structure shown in Figure 1. Selected interatomic distances and bond angles are listed in Table 2. The anionic metallo complex of **1** is

(15) TEXSAN: *Single-Crystal Structure Analysis Software*, Version 5.0; Molecular Structure Corp.: The Woodlands, TX, 1989.

(16) (a) Sheldrick, G. M SHELXS-86: Structure Solving Program; University of Göttingen, Germany, 1986. (b) Sheldrick, G. M SHELXL-93: Structure Refinement Program; University of Göttingen, Germany, 1993.

centrosymmetric and exhibits a distorted octahedral coordination of the two citrate ligands around manganese. The citrate ligands are triply deprotonated. As such, they coordinate to the manganese ion, fulfilling its octahedral coordination requirements. Specifically, each citrate employs the central hydroxyl and carboxylate moieties as well as one of the terminal carboxylates to bind manganese. The remaining carboxylate group is uncoordinated, dangling away from the complex. The Mn−O distances for **1** are similar to those observed in $Mn^{II}(C_4H_4O_5)\cdot 3H_2O$ (2.111−2.220 Å),[17] $Mn^{II}(C_7H_3NO_5)(H_2O)_2$ (2.124(3)−2.262(1) Å),[18] $Mn^{II}(C_2H_3O_3)_2\cdot 2H_2O$ (2.124(3)−2.225(3) Å),[19] $[Mn^{II}(XDK)(NO_3)(CH_3OH)_4(H_2O)_2](NO_3)$ (2.116(2)−2.345(2) Å)[20] (H_2XDK = *m*-xylylenediamine bis(Kemp's triacid imide)), and $[Mn^{II}(bpca)_2\{Mn^{II}(hfac)_2\}_2]$ (2.113(3)−2.190(2) Å)[21] (Hbpca = bis(2-pyridylcarbonyl)amine; Hhfac = hexafluoroacetylacetone), where oxygen-containing octahedral coordination is the predominant feature of the structure around the Mn^{2+} ion. The only other manganese−citrate complex known to date is the polymeric complex $[Mn^{II}(H_2O)_6][Mn^{II}(C_6H_5O_7)(H_2O)]_2\cdot 2H_2O$.[14] The Mn−O distances observed in the complex between the tridentate citrate and Mn^{2+} are comparable to those seen in **1** and range from 2.123(2) to 2.224(2) Å. Further perusal of the literature reveals that **1** is isostructural with the Zn^{2+},[22] Cu^{2+},[23] and Ni^{2+}[24] analogues. The M−O distances observed in the zinc and nickel complexes compare favorably with those seen in **1** and are in the ranges 2.052(2)−2.164(2) Å (Zn^{2+}) and 2.021(3)−2.072(3) Å (Ni^{2+}), while a wider range due to Jahn−Teller distortion is observed in the copper analogue (1.969(3)−2.341(3) Å).

The angles observed around the manganese ion in **1** range from 87.01(6) to 92.99(6)° within the tetragonal plane defined by O(1), O(5), O(1′), and O(5′) and from 72.47(5) to 107.53(5)° (apical positions), showing the angle variability in the geometry adopted by the citrate around manganese. The aforementioned angles are comparable to those observed in the zinc, copper, and nickel analogues.

The central hydroxyl group is strongly hydrogen-bonded to the deprotonated uncoordinated carboxylate moiety of an adjacent molecule, resulting in a polymeric structure [HO(3)···O(7′) = 1.751(1) Å, O(3)···O(7′) = 2.624(1) Å, O(3)−HO(3)···O(7′) = 175.9(1)°; prime = 1 − *x*, 1 − *y*, −*z*]. The hydrogen-bonding network is further extended by the involvement of the ammonium counterions, which interact with both the coordinated and free carboxylate moieties. Moreover, the hydrogen-bonding interactions of the counterions with the free carboxylate groups on the citrate may further contribute to the enhancement of their stability as well as that of the overall complex.

(b) $[Mn(C_6H_4O_7)_2]^{5-}$ (2). Complex **2** crystallizes in the triclinic space group $P\bar{1}$ with 1 molecule in the unit cell. The structure consists of discrete $[Mn(C_6H_4O_7)_2]^{5-}$ anions with the ORTEP structure shown in Figure 2. Selected interatomic

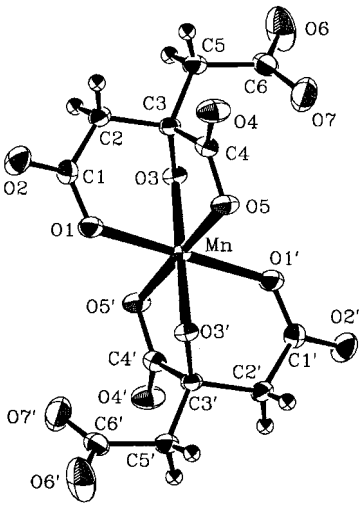

Figure 2. Structure of the $[Mn(C_6H_4O_7)_2]^{5-}$ anion in **2**, along with the atom-labeling scheme. Thermal ellipsoids were drawn by ORTEP and represent 50% probability surfaces.

distances and bond angles are listed in Table 2. The distorted octahedral manganese ion resides on a crystallographic inversion center with the coordinated citrate ligands fully deprotonated. Citrate utilizes, as in the case of the Mn^{2+} congener, the central deprotonated hydroxyl and carboxylate groups as well as one of the terminal carboxylates to achieve octahedral coordination around Mn^{3+}, while the other terminal carboxylate moiety remains uncoordinated, dangling away from the complex.

The Mn−O distances in the coordination sphere of **2** (1.855(1)−2.224(1) Å) are similar to those observed in other high-spin d^4 Mn^{3+} complexes showing Jahn−Teller distortion, such as $[K_2[Mn^{III}(malonate)_2(CH_3OH)_2][Mn^{III}(malonate)_2]]_n$ (1.901(4)−2.262(5) Å),[25] $K_3[Mn^{III}(malonate)_3]\cdot 2H_2O$ (1.923(3)−2.040(3) Å),[26] $[Mn^{III}(C_9H_7NO_3)_2]_2^{2-}$ (1.861(4)−2.236(4) Å),[27] and $[Mn^{III}(MeOH)L(OH)Zn(bpy)]_2\cdot 4$ MeOH (H_4L = 1,2-bis(2-hydroxybenzamido)benzene) (1.901(2)−2.289(3) Å),[28] where the oxygen-containing ligands are bound to the Mn^{3+} ion.

Complex **2** is isostructural with the complexes $[Al(C_6H_4O_7)_2]^{5-}$,[29] $[Fe(C_6H_4O_7)_2]$,[5] $[Ga(C_6H_4O_7)_2]^{3-}$,[30] and $[Cr(C_6H_5O_7)(C_6H_6O_7)]^{2-}$.[30] The octahedral environment in **2** is less distorted than that in **1**, with the ideal 90° angles ranging only between 83.98(6) and 96.02(6)°.

The ammonium counterions balancing the anionic charges in **2** are hydrogen-bonded to both the coordinated and free carboxylates as well as to the hydroxyl groups of the citrate ligands, while the presence of water molecules of crystallization contributes to an extended hydrogen-bonding network. Here as well, the assembly of hydrogen bonds is likely to be a contributing factor in the overall stability of the molecule.

In both **1** and **2**, the citrate ligand adopts its extended conformation upon binding to manganese. The carbon atoms

(17) Van Havere, W.; Lenstra, A. T. H.; Geise, H. J. *Acta Crystallogr., Sect. B* **1980**, *36*, 3117−3120.
(18) Nathan, L. C.; Doyle, C. A.; Mooring, A. M.; Zapien, D. C.; Larsen, S. K.; Pierpont, C. G. *Inorg. Chem.* **1985**, *24*, 2763−2766.
(19) Lis, T. *Acta Crystallogr., Sect. B* **1980**, *36*, 701−703.
(20) Tanase, T.; Lippard, J. F. *Inorg. Chem.* **1995**, *34*, 4682−4690.
(21) Kajiwara, T.; Tasuku, I. J. *Chem. Soc., Dalton Trans.* **1998**, 3351−3352.
(22) Swanson, R.; Ilsley, W. H.; Stanislowski, A. G. *J. Inorg. Biochem.* **1983**, *18*, 187−194.
(23) Bott, R. C.; Sagatys, D. S.; Lynch, D. E.; Smith, G.; Kennard, C. H. L.; Mak, T. C. W. *Aust. J. Chem.* **1991**, *44*, 1495−1498.
(24) Zhou, Z.-H.; Lin, Y.-J.; Zhang, H.-B.; Lin, G.-D.; Tsai, K.-R. *J. Coord. Chem.* **1997**, *42*, 131−141.
(25) Saadeh, S. M.; Trojan, K. L.; Kampf, J. W.; Hatfield, W. E.; Pecoraro, V. L. *Inorg. Chem.* **1993**, *32*, 3034−3040.
(26) Lis, T.; Matuszewski, J.; Jezowska-Trzebiatowska, B. *Acta Crystallogr., Sect. B* **1977**, *33*, 1943−1946.
(27) Tamura, H.; Ogawa, K.; Nakahara, A. *Inorg. Chim. Acta* **1984**, *92*, 107−111.
(28) Sunatsuki, Y.; Shimada, H.; Matsuo, T.; Nakamura, M.; Kai, F.; Matsumoto, M.; Re, N. *Inorg. Chem.* **1998**, *37*, 5566−5574.
(29) Matzapetakis, M.; Raptopoulou, C. P.; Terzis, A.; Lakatos, A.; Kiss, T.; Salifoglou, A. *Inorg. Chem.* **1999**, *38*, 618−619.
(30) (a) Matzapetakis, M.; Raptopoulou, C. P.; Tsohos, A.; Papaefthymiou, V.; Moon, N.; Salifoglou, A. *J. Am. Chem. Soc.* **1998**, *120*, 13266−13267. (b) O'Brien, P.; Salacinski, H.; Motevalli, M. *J. Am. Chem. Soc.* **1997**, *119*, 12695−12696. (c) Quiros, M.; Goodgame, D. M. L.; Williams, D. J. *Polyhedron* **1997**, *11*, 1343−1348.

C(1), C(2), C(3), C(5), and C(6) of the citrate backbone are coplanar, with the largest standard deviations being 0.056 and 0.067 Å for C(3) in **1** and **2**, respectively. The central carboxylate plane O(4)−C(4)−O(5) is rotated ∼10° out of the O(3)−C(3)−C(4) plane in both **1** and **2**, suggesting similar approaches of the citrate ions to the metal ions.

No outstanding differences were observed in the respective C−O and C−C distances of the citrate ligands coordinated to the manganese ions in complexes **1** and **2**. A pronounced difference, however, between **1** and **2** was evident in the protonation states of the citrate ligands coordinated to the metal ions. Specifically, in complex **1**, a proton was present on the central hydroxyl group attached to the metal ion. That proton was absent in the case of **2**, leading to a considerable increase in the Mn−O(3) distance (from 1.885(1) Å in **2** to 2.225(2) Å in **1**). This increase cannot be explained by the difference of ∼0.1 Å between the ionic radii of Mn^{3+} and Mn^{2+}.

Electronic Spectroscopy. The UV/visible spectroscopy of complex **2** was conducted in an aqueous solution at pH ∼7. The electronic spectrum shows a band at 428 nm ($\epsilon = 170$ M^{-1} cm^{-1}), a shoulder descending into lower energies around 520 nm ($\epsilon \sim 59$ M^{-1} cm^{-1}), and a broad band at 730 nm ($\epsilon = 25$ M^{-1} cm^{-1}). The bands are reasonably attributed to d−d transitions on the basis of their low extinction coefficients.[31,32] Because the ground term of a d^4 high-spin octahedral environment, such as the one in complex **2**, is ^5E_g, the degeneracy of the latter is lifted by the Jahn−Teller effect, ultimately leading to a tentative assignment of the observed bands to the transitions $^5B_{1g} \rightarrow {}^5E_g$, $^5B_{1g} \rightarrow 5B_{2g}$ and $^5B_{1g} \rightarrow {}^5A_{1g}$, respectively.

The spin- and parity-forbidden transitions of the high-spin complex **1** are very weak,[31] being hardly observable. The spectrum of **1** in water at pH ∼7 is featureles in the visible region with a sharply ascending absorption into the UV region leading to a band at 200 nm ($\epsilon = 950$ M^{-1} cm^{-1}), most likely reflecting an LMCT absorption.

FT-IR Spectroscopy. The FT-IR spectra of **1** and **2** (in KBr) exhibit strong characteristic absorptions for the carbonyls of the citrate carboxylate ligands in the asymmetric and symmetric vibration regions. Specifically, asymmetric stretching vibrations $\nu_{as}(COO^-)$ appear between 1621 and 1586 cm^{-1} for **1** and between 1636 and 1596 cm^{-1} for **2** and the symmetric stretching vibrations $\nu_s(COO^-)$ are observed between 1436 and 1386 cm^{-1} for **1** and between 1441 and 1397 cm^{-1} for **2**. All of the bands are shifted to lower frequencies compared to those of free citric acid, denoting the changes in the vibrational status of that ligand upon complexation to manganese. For both complexes **1** and **2**, the differences between the symmetric and asymmetric stretches, Δ ($\nu_{as}(COO^-) - \nu_s(COO^-)$),[33] are on the order of 200 cm^{-1} indicating that carboxylate groups are either free or coordinated to the metal in a monodentate fashion, consistent with the observed X-ray crystal structures of **1** and **2**. The aforementioned assignments are in agreement with previous results for citrate complexes of various metals.[29,30]

Magnetic Susceptibility Data. (a) $[Mn(C_6H_5O_7)_2]^{4-}$ (1). Solid-state magnetic susceptibility data were collected on a powdered sample in a 6.0 kG applied magnetic field and in the temperature range from 6.0 to 278 K. The $\chi_M T$ vs T and χ_M vs T plots are shown in Figure 3A.

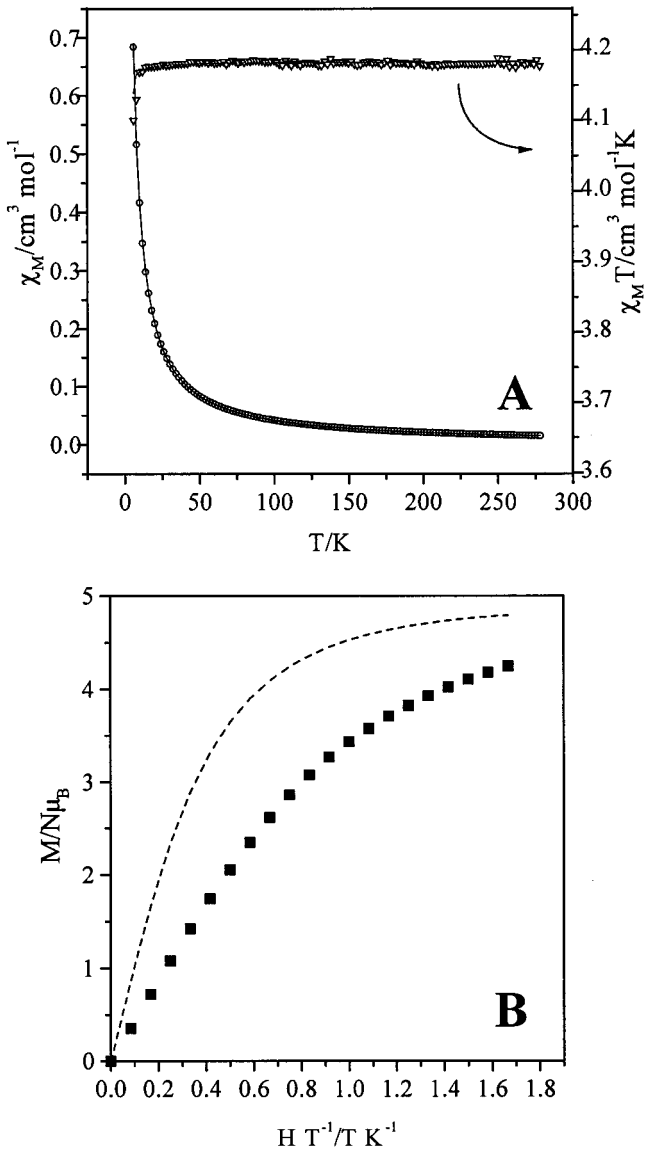

Figure 3. (A) Temperature dependence of the susceptibility data of **1**, in the form of $\chi_M T$ vs T and χ_M vs T plots in a field of 6000 G. The solid line represents the best fit. (B) Reduced magnetization curve, $M/(N\mu_B)$ vs H/T, N = Avogadro's number, for **1** at 5 K and in a 0−5 T field range. The solid line represents the theoretical Brillouin function for an $S = 5/2$ system.

The value of $\chi_M T$ decreases from 4.17 cm^3 mol^{-1} K at 278 K to 4.10 cm^3 mol^{-1} K at 5 K. The high-temperature value of $\chi_M T$ is close to 4.37 cm^3 mol^{-1} K, the value that would be expected for one $S = 5/2$ (high-spin d^5) system. The data are consistent with the presence of an $S = 5/2$ system with an isotropic g of 1.955 and a zero-field splitting, D, of 0.1 cm^{-1}. The data were further analyzed in the high-temperature region (100−295 K) with the Curie−Weiss law, and the fitting procedure gave the values $C = 4.18$ cm^3 mol^{-1} K and $\Theta = 0.08$ K, indicating the paramagnetic nature of the complex.

Magnetization measurements were carried out at 5 K and in the field range 0−5 T. The results are shown in Figure 3B, along with the Brillouin function of an $S = 5/2$ system. The noncoincidence of the two curves is probably due to intermolecular interactions that come into play at very low temperatures.

(b) $[Mn(C_6H_4O_7)_2]^{5-}$ (2). Variable-temperature, solid-state magnetic susceptibility data were collected on a powdered

(31) (a) Vincent, J. B.; Folting, K.; Huffman, J. C.; Christou, G. *Inorg. Chem.* **1986**, *25*, 996−999. (b) Diril, H.; Chang, H.-R.; Nilges, M. J.; Zhang, X.; Potenza, J. A.; Schugar, H. J.; Isied, S. S.; Hendrickson, D. N. *J. Am. Chem. Soc.* **1989**, *111*, 5102−5114.

(32) Lever, A. B. P. *Inorganic Electronic Spectroscopy*, 2nd Ed.; Elsevier: Amsterdam, 1984; pp 443−451.

(33) (a) Djordjevic, C.; Lee, M.; Sinn, E. *Inorg. Chem.* **1989**, *28*, 719−723. (b) Deacon, G. B.; Philips, R. J. *Coord. Chem. Rev.* **1980**, *33*, 227−250.

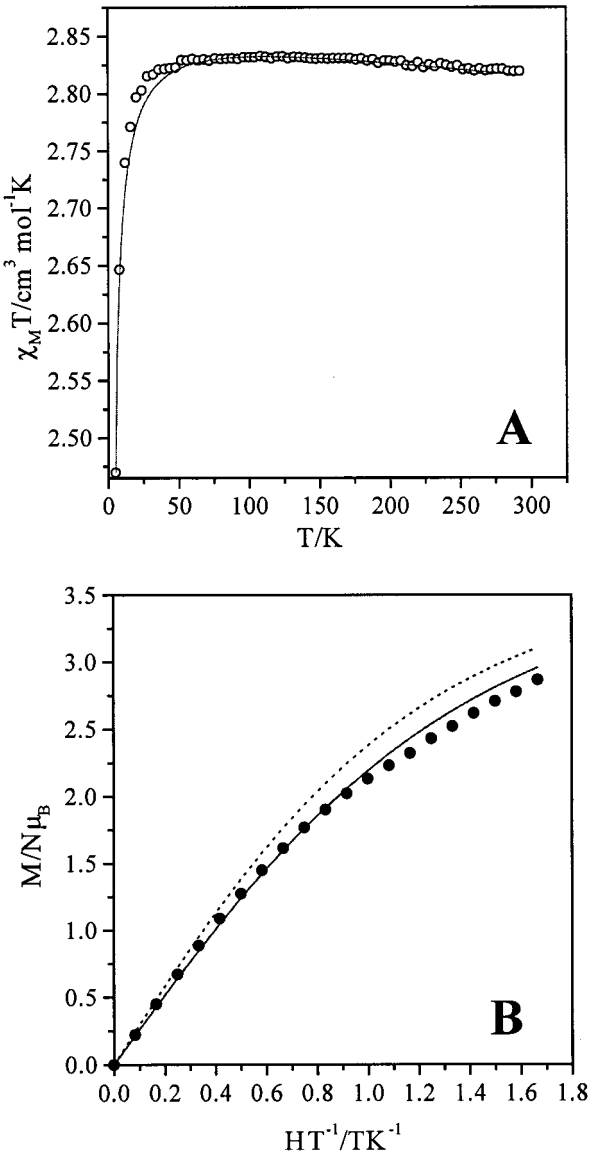

Figure 4. (A) Temperature dependence of the susceptibility data of **2**, in the form of a $\chi_M T$ vs T plot, in a field of 6000 G. The solid line represents the best fit. (B) Reduced magnetization curve, $M/(N\mu_B)$ vs H/T, N = Avogadro's number, for **2** at 5 K and in a 0−5 T field range. The solid line represents the theoretical Brillouin function for an $S = 2$ system with $D = 0.29$ cm^{-1}, while the dotted line represents that for a system with $D = 0$ cm^{-1}.

sample in a 6.0 kG applied magnetic field and in the temperature range 5.0−295 K. The $\chi_M T$ vs T curve is shown in Figure 4A. $\chi_M T$ decreases from 2.82 cm^3 mol^{-1} K at 295 K to 2.47 cm^3 mol^{-1} K at 5 K. The high-temperature value of $\chi_M T$ is close to 3.0 cm^3 mol^{-1} K, the value that would be expected for one $S = 2$ (d^4) system. The data are consistent with $S = 2$, isotropic $g = 1.95$, and a small zero-field splitting of $D = 0.29$ cm^{-1}. In the high-temperature region (100−295 K), the data were analyzed with the Curie−Weiss law, and the fitting procedure gave $C = 2.76$ cm^3 mol^{-1} K and $\Theta = -1.43$ K.

Here as well, magnetization measurements were carried out at 5 K and in the field range 0−5 T. The data were fit to a Brillouin function of an $S = 2$ system with $D = 0.29$ cm^{-1} and $g = 1.93$, and the results are shown in Figure 4B.

EPR Spectroscopy. EPR spectra of both **1** and **2** were recorded at 4 K (Figure 5). The spectrum of the high-spin Mn^{2+} species in **1** at 4 K consists of many features in both the low- and high-field regions. The g values observed are 21.4, 5.34,

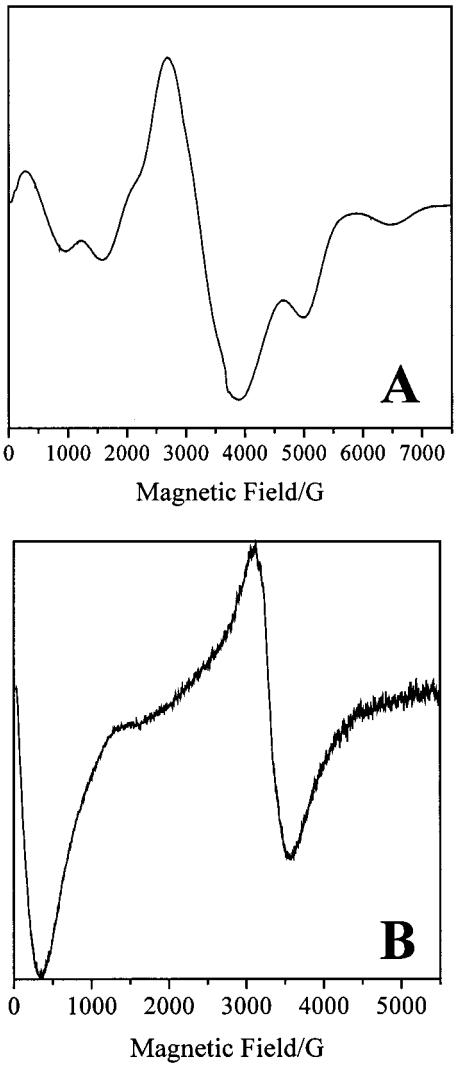

Figure 5. X-Band EPR powder spectra of **1** (A) and **2** (B) at 4 K.

3.18, 2.01, 1.34, and 1.03. This complex spectrum is in line with the results of the magnetic studies and the derived value of the D parameter. Furthermore, as described elsewhere,[34] such spectra are very common for weakly coupled Mn^{2+} derivatives and correspond to the superposition of spectra of the various excited spin states ($S = 1-5$) of the Mn^{2+} pair modulated by a Boltzmann distribution. Nevertheless, contributions from the first and second excited states can be clearly identified in the spectrum.

While, in most cases, the Mn^{3+} ion is EPR "silent",[35] this is one of the rare cases where we were able to obtain an EPR spectrum of complex **2** on a conventional X-band spectrometer (where $B_1 \perp B$). The lack of signals in most cases is presumably explained by the magnitudes of zero-field parameters, which shift the EPR resonance out of the energy regime of an X-band spectrometer; $\Delta > h\nu < \sim 0.3$ cm^{-1}. In our case, the zero-field parameter obtained from the magnetic measurements is smaller than the microwave energy, thus giving rise to an interesting absorption located at $g = 43.7$, which is attributed to an integer-spin system, along with a central feature at $g = 2.0$. It is quite difficult to attribute this central signal to the S = 2 system, and

(34) Khangulov, S. V.; Barynin, V. V.; Voevodskaya, N. V.; Grebenko, A. I. *Biochim. Biophys. Acta* **1990**, *1020*, 305−310.
(35) Goldberg, D. P.; Telser, J.; Krzystek, J.; Montalban, A. G.; Brunel, L.-C.; Barrett, A. G. M.; Hoffman, B. M. *J. Am. Chem. Soc.* **1997**, *121*, 8722−8723.

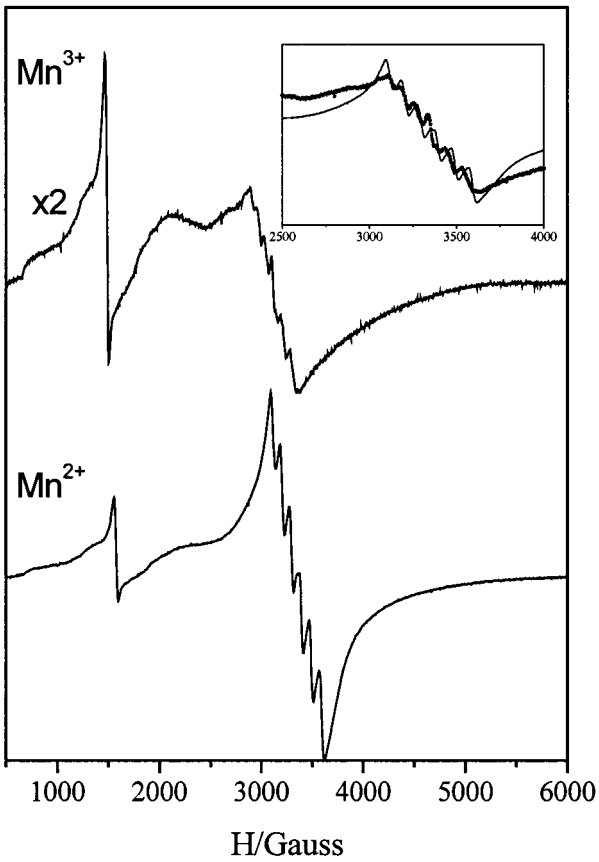

Figure 6. X-Band EPR spectra of **1** and **2** in water (~9 mM) at room temperature (pH ~7). In the inset, the difference in the hyperfine splitting is shown, where the dotted line represents the hyperfine splitting of Mn^{3+} complex **2** and the solid line that of the Mn^{2+} complex **1**.

a small percentage of Mn^{2+} may be responsible for this. It should be pointed out that similar spectra have been observed elsewhere[36] (in the case of the $FeSO_4$ $S = 2$ system), where the presence of a $g = 2$ signal was attributed to a ferric impurity.

EPR experiments were also conducted for compounds **1** and **2** in aqueous solutions. The EPR spectra of the respective Mn^{2+} and Mn^{3+} complexes are shown in Figure 6. The hyperfine structures of the complex ions in **1** and **2** are clearly resolved, as is the difference in the spectral intensities. The spectrum of the Mn^{3+} complex is centered at $g = 2.0$, and its intensity is 20% of the intensity of the spectrum for the analogous Mn^{2+} complex. Moreover, unlike Mn^{2+} in **1**, which exhibits an isotropic hyperfine structure ($A = 100$ G), Mn^{3+} in **2** exhibits an anisotropic hyperfine structure (inset of Figure 6). Other observed resonances for both **1** and **2** are centered at $g = 4.2$ and 2.9. The difference between the spectra of the two complexes is clearly seen in Figure 7, where the EPR spectra are displayed for **1** and **2** at 4 K. The spectrum of the Mn^{3+} complex reveals resonances at $g = 30.0$, 7.86, 2.65, and 2.0 (suggesting again the integer character of the ground state), while, in the case of the Mn^{2+} spectrum, a single resonance is observed at $g = 2$. Overall, the EPR results indicate that the two complexes retain their structures in aqueous solution.

Discussion

The syntheses of **1** and **2** in aqueous solutions, their isolations, and their spectroscopic and structural characterizations provide

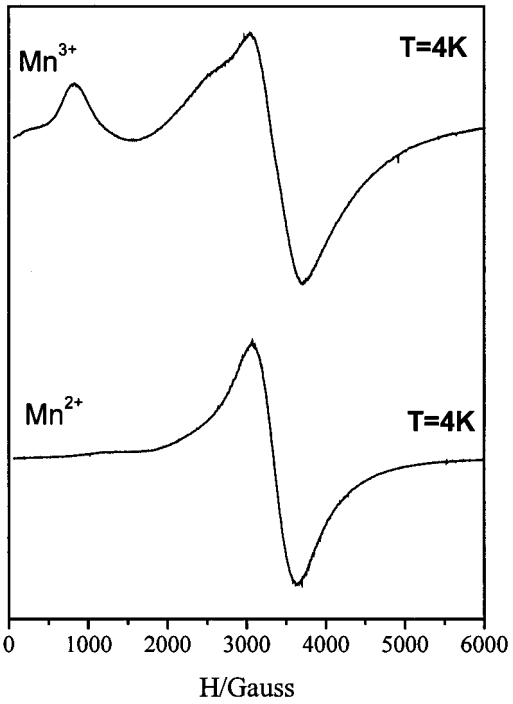

Figure 7. X-Band EPR spectra of **1** and **2** in water (pH ~7) at 4 K.

clear cases of mononuclear manganese species bearing the biologically relevant binder citrate. It appears that interactions of citrate with manganese, according to a pH-sensitive protocol, lead to octahedral complexes in which the modes of citrate binding to the metal ion in two different oxidation states are the same. What emerges as a differentiating factor for the complexes is the protonation state of the citrate ligand in conjunction with the oxidation state of the metal ion to which it is attached. In the first case, Mn^{2+} coordinates to the triply deprotonated citrate, whereas, in the second case, coordination to Mn^{3+} requires the fully deprotonated citrate, created by the additional removal of the central hydroxyl hydrogen. It is worth emphasizing that **2** is a rare example of a complex with polycarboxylate ligands coordinated to Mn^{3+}. It has been reported that polycarboxylate ligands are subject to oxidative decarboxylation in the presence of Mn^{3+}.[37] In our case, a preliminary investigation of the synthesis mixture for reaction 2 indicates that, in addition to citrate, keto species are also present, possibly contributing to the lower than quantitative synthetic yields for complex **2**.[38] Despite the idiotypic chemical behavior of the Mn^{3+}−citrate system, under the employed synthesis conditions, complex **2** is isolated in a fairly good yield and is a stable compound.

The EPR spectroscopic studies of **1** and **2** show that both complexes exist as mononuclear soluble entities in aqueous solutions of pH ~7. As such, **1** and **2** represent low molecular weight species potentially capable of influencing the chemistry of manganese in biological fluids. The latter statement assumes greater significance in light of that metal ion's purported ability to act (a) as an essential element in the normal development and function of the brain[10b,39] and (b) as a neurotoxicant,[40] above

(36) Hendrich, M. P.; Debrunner, P. G. *Biophys. J.* **1989**, *56*, 489−506.

(37) (a) Urzua, U.; Kersten, P. J.; Vicuna, R. *Arch. Biochem. Biophys.* **1998**, *360*, 215−222. (b) Mukhopadhyay, S.; Chaudhury, S.; Das, R.; Banerjee, R. *Can. J. Chem.* **1993**, *71*, 2155−2159. (c) Datta, S. P.; Grzybowski, A. K.; Tate, S. S. *Nature* **1965**, 1047−1049.

(38) Friedemann, T. E.; Haugen, G. E. *J. Biol. Chem.* **1943**, *147*, 415−441.

(39) Rabin, O.; Hegedus, L.; Bourre, J.-M.; Smith, Q. R. *J. Neurochem.* **1993**, *61*, 509−517.

and beyond its conventional metalloenzymic participation, rendering biological sites in the brain prone to neurodegeneration and pathophysiological aberrations (e.g., idiopathic Parkinson's disease).[12] The results reported here are in accord with those from past potentiometric pH studies of Mn^{2+}−citrate systems,[41] supporting the existence of mononuclear Mn^{2+}−citrate species having various protonation states for the citrate binder. To our knowledge, no similar studies exist for the analogous Mn^{3+}−citrate systems in aqueous solutions. Undoubtedly, such work is needed for comparison with the results reported herein for the mononuclear Mn^{3+} species.

It is known that most metals gain access to the brain through the blood. Therefore, their uptakes are significantly influenced by their forms as well as their speciations and concentrations. Metal ion uptake is thought to be facilitated by primary serum binding proteins, prominent among which is the transferrin molecule, also essential for Fe^{3+}, as well as small molecular weight complexes. Despite their presence at low concentrations in plasma, the contributions of the latter species in pathways leading to the uptake of manganese should not be discounted, as conditions in the serum are amenable to changes, accordingly dictating manganese's speciation and likely promoting varying interactions with citrate. Citrate is known to be a multimodal natural metal ion binder occurring physiologically at noticeable concentrations (∼0.1 mM). Thus, citrate's ability to solubilize manganese in complex forms similar to those of **1** and **2** near physiological pH values may be responsible for its action as a mobilizer and its contribution as an organic cofactor to the ultimate absorption of manganese by biological sites.

The two complexes contain manganese in two oxidation states, both of which have been found to be present in living tissue.[42] Mn^{2+} has been found to bind, following uptake, to the inner membrane of brain mitochondria, where electron transport occurs. Mn^{3+} can readily coordinate to the transferrin molecule, presumably by binding to it in a manner analogous to that of Fe^{3+}. The formation of this system provides a transferrin-dependent pathway for the entrance of manganese into the central nervous system via effective crossing of the blood−brain barrier. Finally, the importance of catecholamines[42] in mobilizing Mn^{3+} ions and enhancing their availability to sites of oxidative damage has also been reported, lending credence to the aforementioned proposal that complexes **1** and **2** may be potential species for exemplifying the chemical reactivity of manganese in biological fluids.

Even though the charges borne by the anionic complexes in **1** and **2** are high (4− and 5−, respectively), the mononuclear species present credible forms of solubilized manganese ions in biologically relevant oxidation states. It would, undoubtedly, be desirable for the complexes to bear charges lower than those reported herein if such species were to be involved in the crossing of the blood−brain barrier. Previous solution studies addressing the nature of Mn^{2+}−citrate species in aqueous solutions as a function of pH strongly suggested the presence of species such as $[Mn^{II}Cit]^{2-}$, $[Mn^{II}Cit]^{-}$, and $[Mn^{II}Cit]^{0}$.[41] Consequently, complexes like the aforementioned or $[Mn^{III}(Cit)_2]^{3-}$ would be more relevant to species that are increasingly more mobile and possibly more readily absorbable by biological tissues. An investigation of such complexes of manganese with citrate as well as their pH- and concentration-dependent behavior in aqueous solutions may help to delineate details of the manganese(2+/3+) speciation and incipient role(s) in biological fluids. These studies are currently being conducted in our laboratories.

Acknowledgment. This work was supported with funds provided by the Department of Chemistry, University of Crete, Greece (Grant ELKE 1186). We are also grateful to the Agricultural Bank of Greece and Mr. John Boutaris for providing financial support to C.P.R. and A.T.

Supporting Information Available: X-ray crystallographic files, in CIF format, and listings of positional and thermal parameters and H-bond distances and angles for **1** and **2** and a UV/vis spectrum of **2**. This material is available free of charge via the Internet at http://pubs.acs.org.

IC9912631

(40) (a) Aschner, M.; Aschner, J. L. *Neurosci. Biobehav. Rev.* **1991**, *15*, 333−340. (b) Donaldson, J. *Neurotoxicology* **1987**, *8*, 451−462.

(41) (a) Grzybowski, A. K.; Tate, S. S.; Datta, S. P. *J. Chem. Soc., Sect. A* **1970**, 241−245. (b) Shnarevich, A. I. *Russ. J. Inorg. Chem. (Engl. Transl.)* **1963**, *8*, 1083−1086. (c) Li, N. C.; Lindenbaum, A.; White, J. M. *J. Inorg. Nucl. Chem.* **1959**, *12*, 122−128. (d) Wiberg, J. S. *Arch. Biochem. Biophys.* **1958**, *73*, 337−385.

(42) Archibald, F. S.; Tyree, C. *Arch. Biochem. Biophys.* **1987**, *256*, 638−650.